Theory of diffusion of active particles that move at constant speed in two dimensions

Francisco J. Sevilla[1,*] and Luis A. Gómez Nava[1,2]

[1]*Instituto de Física, Universidad Nacional Autónoma de México, Apartado Postal 20-364, 01000 México Distrito Federal, Mexico*

[2]*Posgrado en Ciencias Físicas, Universidad Nacional Autónoma de México, Circuito de Posgrados, Ciudad Universitaria, Coyoacán, 04510 México Distrito Federal, Mexico*

(Received 2 May 2014; published 25 August 2014)

Starting from a Langevin description of active particles that move with constant speed in infinite two-dimensional space and its corresponding Fokker-Planck equation, we develop a systematic method that allows us to obtain the coarse-grained probability density of finding a particle at a given location and at a given time in arbitrary short-time regimes. By going beyond the diffusive limit, we derive a generalization of the telegrapher equation. Such generalization preserves the hyperbolic structure of the equation and incorporates memory effects in the diffusive term. While no difference is observed for the mean-square displacement computed from the two-dimensional telegrapher equation and from our generalization, the kurtosis results in a sensible parameter that discriminates between both approximations. We carry out a comparative analysis in Fourier space that sheds light on why the standard telegrapher equation is not an appropriate model to describe the propagation of particles with constant speed in dispersive media.

DOI: 10.1103/PhysRevE.90.022130 PACS number(s): 02.50.−r, 05.40.−a, 02.30.Jr

I. INTRODUCTION

The study of transport properties of active (self-propelled) particles has received much attention during the past two decades [1,2]. Self-propulsion, as a feature of systems out of equilibrium, has been introduced in a variety of contexts to describe the foraging of organisms in ecology problems [3,4], the motion of bacteria [5], and photon migration in multiple scattering media [6–8], just to name a few. More recently self-propulsion was incorporated into micron-sized particles by conversion of chemical energy into self-phoretic motion [9,10].

A simple model for self-propulsion is to consider that the particles move with constant speed in a manifold of interest, which in many cases coincides with the two-dimensional space. This simplified modeling of particle activation has been approximately supported by experimental studies in many real biological systems [11–16] and has been used in several theoretical studies of systems that exhibit collective motion [17,18] for interacting self-driven particles, anomalous diffusion [19] when particles move in heterogeneous landscapes, and motion persistence [20–22] if the particles are under the influence of fluctuating torques.

Previous studies on diffusion theory within the framework of random walks used persistent random walks (see [23], and references therein) and their phenomenological generalizations [24] to incorporate internal states, which sometimes are related to kinematic properties of the walker, such as velocity. Generally, the interest lies in a coarse-grained description of the probability density $P(\boldsymbol{x},t)$ of finding a particle at position $\boldsymbol{x}$ at time t, for which the detailed information about the internal states is irrelevant. As a standard procedure, the limit of the continuum is taken, which leads to a partial differential equation (PDE) for $P(\boldsymbol{x},t)$. Depending on the spatial dimension, those PDEs are reminiscent of the well-known diffusion equation. For instance, the one-dimensional persistent random walk leads to the telegrapher equation (TE) whose solution corrects, in the short-time regime, the infinite speed of signal propagation exhibited by the solution to the diffusion equation. In fact, the solution to the TE shows a transition from a wavelike behavior at short times to a diffusive behavior in the long-time regime (see [25], and references therein).

That dimensionality plays a significant role in various physical phenomena has been pointed out by many authors (see Ref. [26], and references therein), particularly regarding the transmission of information described by the wave equation, which favors three dimensions for signal fidelity transmission, a feature desired as part of an anthropic principle. By contrast, the solution to the two-dimensional wave equation presents signal reverberation, making impossible the transmission of sharply defined signals. In additional, such a solution is negative for points inside the propagating front if initial data correspond to an impulse with zero velocity [27].

Generalizations of the persistent random walk to arbitrary dimension d greater than one have been formulated [28]; however, physical interpretation of the PDE obtained after taking the limit of the continuum is hindered due to the presence of partial derivatives of order $2d$. This departure from the one-dimensional case, which contains at most partial derivatives of order 2, is conspicuously important in the short-time regime. Thus deriving an appropriate transport equation for the coarse-grained probability distribution in dimensions larger than one has been a central issue [24,29–31].

The description of particles that move with constant speed is also susceptible to the spatial dimension of the system and one dimension seems to be particularly exceptional regarding the TE since this has been derived exactly from various equivalent *microscopic* models [32–34] that consider the random transitions between the velocity states $\pm c$ (also known as the Goldstein-Kac process; see Ref. [35]), namely,

$$\frac{\partial^2}{\partial t^2}P(x,t)+\gamma\frac{\partial}{\partial t}P(x,t)=c^2\frac{\partial^2}{\partial x^2}P(x,t), \qquad (1)$$

*Author to whom correspondence should be addressed: fjsevilla@fisica.unam.mx

where γ is the transition rate between the internal states $\pm c$. A generalization of this dichotomic process to dimensions larger than one has lead to a fourth-order PDE [7] for particles that move with constant speed $\sqrt{2}c$ along the diagonals of a square lattice in two dimensions. The straightforward generalization to $d > 1$ spatial dimensions $\partial_t^2 P + \gamma \partial_t P = c^2 \nabla_d P$ has been considered before in the context of photon propagation in turbid media [36–38]; however, it does not always result in an appropriate physical interpretation as already discussed in Refs. [25,39,40], particularly in two dimensions, since at short times the wavelike behavior implies that the particle probability density becomes negative.

In this work we present an analysis of Brownian-like particles that move with constant speed in infinite two-dimensional space and whose trajectories are obtained from Langevin-like equations. Through suitable transformations of the Fokker-Planck equation for $P(\boldsymbol{x},\varphi,t)$, with φ the internal state that gives the direction of motion of a single particle, we are able to obtain approximate diffusionlike equations for the coarse-grained probability distribution $P(\boldsymbol{x},t)$. As expected, the TE is obtained in the long-time limit and a generalization of it is obtained by describing the system in a shorter-time regime. This generalization incorporates memory functions and keeps the hyperbolic nature of the original TE.

In Sec. II we provide the Langevin equations for the trajectories of particles that move with constant velocity and the Fokker-Planck equation for the probability density $P(\boldsymbol{x},\varphi,t)$ of a particle being at point $\boldsymbol{x}$, moving in direction φ at time t as stated. In Sec. III we present our method of analysis and derive a generalization of the TE. A comparative analysis of the generalized and the original TE is given in Sec. IV. We summarize in Sec. V.

II. LANGEVIN EQUATIONS FOR BROWNIAN AGENTS WITH CONSTANT SPEED

The kinematic state of a constant speed particle at time t is determined by its position $\boldsymbol{x}(t)$ and the direction of motion $\hat{\boldsymbol{v}}(t)$. In additional, the particles are subject to the influence of stochastic fluctuations that only affect the direction of motion. The time evolution of the particle's state is given by the Langevin equations

$$\frac{d}{dt}\boldsymbol{x}(t) = v_0 \hat{\boldsymbol{v}}(t), \tag{2a}$$

$$\frac{d}{dt}\varphi(t) = \xi(t), \tag{2b}$$

where the instantaneous unitary vector $\hat{\boldsymbol{v}}(t)$ is given by $[\cos\varphi(t), \sin\varphi(t)]$, $\varphi(t)$ being the instantaneous angle between the direction of motion and the horizontal axis. These equations describe the motion of a Brownian particle that moves with constant speed and rotates its direction of motion due to Gaussian white noise $\xi(t)$, i.e., $\langle\xi\rangle = 0$ and $\langle\xi(t)\xi(s)\rangle = 2\gamma\delta(t-s)$, where γ is a constant that has units of $[\text{time}]^{-1}$ and denotes the intensity of the noise. More precisely, Eq. (2b) is the two-dimensional version of the general relation $d\hat{\boldsymbol{v}}(t)/dt = \boldsymbol{\xi}(t) \times \hat{\boldsymbol{v}}(t)$, which gives the rotational dynamics of the unitary vector $\hat{\boldsymbol{v}}$ in three dimensions, caused by the fluctuating angular acceleration $\boldsymbol{\xi}$. Throughout this paper we consider quantities with explicit time dependence to denote those stochastic processes that appear in the Langevin equations (2), reserving the use of quantities without the explicit temporal dependence to appear in the corresponding Fokker-Planck equation.

Though active agents do not strictly move with constant speed, fluctuations around the average value are small, as occurs in systems of micron-sized Janus particles [9,41] whose speed values varies from 10^{-2} to 10^{-1} $\mu\text{m s}^{-1}$ [41] or several $\mu\text{m s}^{-1}$ [9], depending on the method to extract the particle speed from trajectory data. In the same experiments, the other parameter of our model, namely, the time scale γ^{-1}, varies from several seconds in Ref. [9] to approximately 2×10^2 s in structured environments [41].

From Eqs. (2) we obtain the following equation for the one-particle probability density $P(\boldsymbol{x},\varphi,t) \equiv \langle\delta(\boldsymbol{x} - \boldsymbol{x}(t))\delta(\varphi - \varphi(t))\rangle$:

$$\frac{\partial}{\partial t}P(\boldsymbol{x},\varphi,t) + v_0\hat{\boldsymbol{v}}\cdot\nabla P(\boldsymbol{x},\varphi,t) = -\frac{\partial}{\partial\varphi}\langle\xi(t)\delta(\boldsymbol{x} - \boldsymbol{x}(t))\delta(\varphi - \varphi(t))\rangle, \tag{3}$$

where $\langle\cdot\rangle$ denotes the average over noise realizations. After making use of Novikov's theorem we get the Fokker-Planck equation

$$\frac{\partial}{\partial t}P(\boldsymbol{x},\varphi,t) + v_0\hat{\boldsymbol{v}}\cdot\nabla P(\boldsymbol{x},\varphi,t) = \gamma\frac{\partial^2}{\partial\varphi^2}P(\boldsymbol{x},\varphi,t). \tag{4}$$

In this expression we have omitted the term $-v_0\nabla\cdot\langle[\int_0^t ds\,\hat{\boldsymbol{v}}(s)]\delta(\boldsymbol{x} - \boldsymbol{x}(t))\delta(\varphi - \varphi(t))\rangle$, assuming that the integral within parentheses vanishes at all times. Equation (4) has also been derived from equivalent arguments in Ref. [8].

By performing the Fourier transform over the spatial coordinates and performing the Fourier expansion with respect to the angle φ, we transform Eq. (4) into the following set of tridiagonal coupled ordinary differential equations for the nth coefficient $\tilde{P}_n(\boldsymbol{k},t)$:

$$\frac{d}{dt}\tilde{P}_n(\boldsymbol{k},t) = -\frac{v_0}{2}[(ik_x + k_y)\tilde{P}_{n-1}(\boldsymbol{k},t) + (ik_x - k_y) \times \tilde{P}_{n+1}(\boldsymbol{k},t)] - \gamma n^2\tilde{P}_n(\boldsymbol{k},t), \tag{5}$$

which satisfies $\tilde{P}_n(\boldsymbol{k},t) = \tilde{P}^*_{-n}(-\boldsymbol{k},t)$ and is given by $(2\pi)^{-2}\int d^2\boldsymbol{x}\int_0^{2\pi} d\varphi\, e^{i(\boldsymbol{k}\cdot\boldsymbol{x} - n\varphi)}P(\boldsymbol{x},\varphi,t)$. We are interested in the solution of (5) with the initial condition $\tilde{P}_n(\boldsymbol{k},0) = \delta_{n,0}/2\pi$, which corresponds to the initial condition $P(\boldsymbol{x},\varphi,0) = \delta^{(2)}(\boldsymbol{x})/2\pi$, where $\delta_{n,m}$ and $\delta^{(2)}(\boldsymbol{x})$ denote the Kronecker delta and the two-dimensional Dirac delta, respectively. Through a further transformation, namely,

$$\tilde{P}_n(\boldsymbol{k},t) = e^{-\gamma n^2 t}\tilde{p}_n(\boldsymbol{k},t), \tag{6}$$

we obtain the one-step process with nonlinear coefficients

$$\frac{d}{dt}\tilde{p}_n = -\frac{v_0}{2}[(ik_x + k_y)e^{-\gamma(-2n+1)t}\tilde{p}_{n-1} + (ik_x - k_y)e^{-\gamma(2n+1)t}\tilde{p}_{n+1}], \tag{7}$$

where the arguments of $\tilde{p}_n$ have been omitted for clarity. Although Eq. (7) can be solved in principle by the method of continued fractions [42], we are interested in a coarse-grained description of the system in which the direction of motion of the particle is not relevant. Thus we focus on the probability density distribution $P_0(\boldsymbol{x},t) \equiv (2\pi)^{-1}\int d^2\boldsymbol{k}\, e^{-i\boldsymbol{k}\cdot\boldsymbol{x}}\tilde{p}_0(\boldsymbol{k},t) = \int_0^{2\pi} d\varphi\, P(\boldsymbol{x},\varphi,t)$. The explicit appearance of the exponential factors in Eq. (7) makes it clear that they are suitable to perform an analysis of different time regimes for $P_0(\boldsymbol{x},t)$, which initiates in the diffusive limit (long-time regime) and extends to consider shorter times.

III. GENERALIZATION OF THE TELEGRAPHER EQUATION

Let us first consider the long-time regime or diffusive limit $3\gamma t \gg 1$ for which we only hold the three Fourier coefficients $n = 0,\pm1$ in Eq. (7), i.e.,

$$\frac{d}{dt}\tilde{p}_0 = -\frac{v_0}{2}e^{-\gamma t}[(ik_x + k_y)\tilde{p}_{-1} + (ik_x - k_y)\tilde{p}_1], \quad (8a)$$

$$\frac{d}{dt}\tilde{p}_{\pm1} = -\frac{v_0}{2}e^{\gamma t}(ik_x \pm k_y)\tilde{p}_0, \quad (8b)$$

and by eliminating $p_{\pm1}$ one can show straightforwardly that $P_0(\boldsymbol{x},t)$ satisfies the TE

$$\frac{\partial^2}{\partial t^2}P_0(\boldsymbol{x},t) + \gamma\frac{\partial}{\partial t}P_0(\boldsymbol{x},t) = \frac{v_0^2}{2}\nabla^2 P_0(\boldsymbol{x},t), \quad (9)$$

which agrees with the diffusive limit obtained in Ref. [39] in the context of a transport equation that considers the scattering of the direction of motion. This result is well known and corresponds to our first approximation to the problem. Equation (9) describes wavelike propagation in the short-time regime of pulses that travel not with speed v_0 but diminished by the factor $1/\sqrt{2}$, as is well known. In the asymptotic limit $\gamma t \to \infty$, the dispersive term dominates over the inertial one, given by the second-order partial derivative with respect t, and Eq. (9) reduces to the diffusion equation with diffusion constant $D = v_0^2/2\gamma$. The solution to Eq. (9) is given explicitly in Refs. [27,39] and is solved under standard boundary conditions at infinity $P_0(\boldsymbol{x},t)|_{|\boldsymbol{x}|\to\infty} \to 0$ and under the initial conditions $P_0(\boldsymbol{x},0) = \delta^{(2)}(\boldsymbol{x})$ and $\partial_t P_0(\boldsymbol{x},0) = 0$, which are derived from the initial conditions for Eq. (5); the latter arises exactly from the coarsening procedure. In the wave-vector domain, the solution to (9) is simple and the same for arbitrary dimension d, given by $\tilde{P}_0(\boldsymbol{k},0)e^{-\gamma t/2}(\gamma \sin\omega_{k_d}t/2\omega_{k_d} + \cos\omega_{k_d}t)$ with $\omega_{k_d}^2 \equiv c_d^2k_d^2 - \gamma^2/4$ and $c_d \equiv v_0/\sqrt{d}$, k_d the speed of propagation and the norm of the wave vector in d dimensions. At short times, the expression can be approximated by $\tilde{P}_0(\boldsymbol{k},0)\cos c_d k t$, which corresponds to the normalized solution of the d-dimensional wave equation with initial conditions $\tilde{P}_0(\boldsymbol{k},0), \partial_t\tilde{P}_0(\boldsymbol{k},0) = 0$.

For a description of the system in a shorter-time regime, namely, $5\gamma t \gg 1$, we require the next coefficients $n = \pm2$ of the Fourier expansion to be taken into account; thus from Eq. (7) we get

$$\frac{d}{dt}\tilde{p}_0 = -\frac{v_0}{2}e^{-\gamma t}[(ik_x + k_y)\tilde{p}_{-1} + (ik_x - k_y)\tilde{p}_1], \quad (10a)$$

$$\frac{d}{dt}\tilde{p}_{\pm1} = -\frac{v_0}{2}e^{\gamma t}[(ik_x \pm k_y)\tilde{p}_0 + e^{-4\gamma t}(ik_x \mp k_y)\tilde{p}_{\pm2}], \quad (10b)$$

$$\frac{d}{dt}\tilde{p}_{\pm2} = -\frac{v_0}{2}e^{3\gamma t}(ik_x \pm k_y)\tilde{p}_{\pm1}. \quad (10c)$$

These equations lead to a generalization of the TE for $P_0(\boldsymbol{x},t)$ after eliminating $\tilde{p}_{\pm1}$ from (10a), namely,

$$\frac{\partial^2}{\partial t^2}P_0(\boldsymbol{x},t) + \gamma\frac{\partial}{\partial t}P_0(\boldsymbol{x},t) = v_0^2\nabla^2\int_0^t ds\,\phi(t-s)P_0(\boldsymbol{x},s) + \frac{v_0^2}{4}e^{-4\gamma t}Q(\boldsymbol{x}), \quad (11)$$

where the memory function $\phi(t)$ is given by $\frac{3}{4}\delta(t) - \gamma e^{-4\gamma t}$ and $Q(\boldsymbol{x})$ is a function that is determined from the initial distribution $P(\boldsymbol{x},\varphi,0)$ through

$$\int_0^{2\pi} d\varphi\left[e^{i2\varphi}(\partial_x + i\partial_y)^2 + e^{-i2\varphi}(\partial_x - i\partial_y)^2 - \left(\partial_x^2 + \partial_y^2\right)\right] \times P(\boldsymbol{x},\varphi,0). \quad (12)$$

It can be shown that the initial and boundary conditions for Eq. (11), as derived from those for the detailed probability density $P(\boldsymbol{x},\varphi,t)$, correspond exactly to the initial and boundary conditions for (9).

In the time regime of validity of Eq. (11) we have the following solution in the Fourier-Laplace domain:

$$\hat{P}_0(\boldsymbol{k},\epsilon) = \frac{(\epsilon+\gamma)\tilde{P}_0(\boldsymbol{k},0) + \left(v_0^2/4\right)\tilde{Q}(\boldsymbol{k})/(\epsilon+4\gamma)}{\epsilon^2 + \gamma\epsilon + v_0^2k^2\hat{\phi}(\epsilon)}, \quad (13)$$

where $\hat{\phi}(\epsilon) = 3/4 - \gamma(4\gamma+\epsilon)^{-1}$, ϵ denotes the Laplace variable, and $\hat{f}(\epsilon) = \int_0^\infty dt\, e^{-\epsilon t}f(t)$ is the Laplace transform of $f(t)$. Inversion of the Green's function $G(\boldsymbol{k},\epsilon) = [\epsilon^2 + \gamma\epsilon + v_0^2k^2\hat{\phi}(\epsilon)]^{-1}$ can be done approximately in the time and space regimes $\epsilon \ll 4\gamma$ and $k \ll 4\gamma/v_0$, respectively (see Appendix B), giving for $G(\boldsymbol{x},t)$

$$G(\boldsymbol{x},t) = \frac{8\gamma}{\pi v_0^2}\int d^2\boldsymbol{x}' e^{-(8\gamma/v_0^2t)(\boldsymbol{x}-\boldsymbol{x}')^2}G_{\mathrm{TE}}(\boldsymbol{x}',t), \quad (14)$$

where $G_{\mathrm{TE}}(\boldsymbol{x},t)$ is the corresponding well known Green's function of the TE [27,39].

Though it is possible to go beyond Eq. (11) by considering the following coefficients of the Fourier expansion $n = \pm3$, we point out that partial derivatives of order 4 start to appear in the coarse-grained description and that the memory function $\phi(t)$ becomes more involved, making the analysis more difficult than necessary. As is shown in the following section, Eq. (11) gives an appropriate description of active Brownian particles that move with constant speed, improving the results given by the TE.

IV. DISCUSSION

It has been established that the TE gives a better description of particles that move with constant speed than the diffusion equation [39]. Thus, how much better is the generalization of the former, given by Eq. (11), at shorter times? To answer this question we calculate the mean-square displacement (MSD) and the kurtosis κ for the solutions of Eqs. (9) and (11) and compare them with the exact results from numerical simulations by solving Eqs. (2).

The time dependence of the MSD is generally measured in real systems of active particles [9,10,41,43,44] by use of the single-particle tracking methods [45]. Higher displacement moments, skewness, and kurtosis in one direction have also been determined to quantify the non-Gaussian behavior of the particle distribution [44].

A. Mean-square displacement

A prediction from our analysis is the mean-square displacement $\langle \boldsymbol{x}^2(t)\rangle = \int d^2\boldsymbol{x}\, \boldsymbol{x}^2 P_0(\boldsymbol{x},t) = -(\partial_{kx}^2 + \partial_{ky}^2)\tilde{P}_0(\boldsymbol{k},t)|_{\boldsymbol{k}=0}$. By multiplying by $\boldsymbol{x}^2$ and integrating over the whole space equations (9) and (11), we obtain, respectively,

$$\frac{d^2}{dt^2}\langle \boldsymbol{x}^2(t)\rangle + \gamma \frac{d}{dt}\langle \boldsymbol{x}^2(t)\rangle = 2v_0^2, \tag{15a}$$

$$\frac{d^2}{dt^2}\langle \boldsymbol{x}^2(t)\rangle + \gamma \frac{d}{dt}\langle \boldsymbol{x}^2(t)\rangle = 2v_0^2 + v_0^2 e^{-4\gamma t}(1+\beta/4), \tag{15b}$$

where $\beta = \int d^2\boldsymbol{x}\, \boldsymbol{x}^2 Q(\boldsymbol{x})$. It can be shown that $\beta = -4$ for all smooth circularly symmetric initial distributions (see Appendix A). This observation ensures that the MSD for both approximations shows the same and exact dependence with time, namely,

$$\langle \boldsymbol{x}^2(t)\rangle = \langle \boldsymbol{x}^2(0)\rangle + \frac{4D}{\gamma}[\gamma t - (1-e^{-\gamma t})], \tag{16}$$

for circularly symmetric distributions taken as initial distributions. Thus, the MSD does not provide a measure of the departure between the solution of Eqs. (9) and (11), nor between these and the exact solution obtained from numerical simulations (see Fig. 1). Equations (15) were solved with the initial condition $\frac{d}{dt}\langle \boldsymbol{x}^2(t)\rangle|_{t=0} = 0$, which has been chosen based on the expected physical behavior. Expression (16) coincides with the result obtained by Ornstein [46] and Fürth [47] for the Langevin description of underdamped Brownian motion [48] if v_0 is replaced by $\sqrt{\langle \boldsymbol{v}^2\rangle} = \sqrt{2k_BT/m}$, where k_B is the Boltzmann constant, T the absolute temperature, and m the mass of the particles.

For $\gamma t \ll 1$ the particles show the t^2 dependence that corresponds to the ballistic regime, while for $\gamma t \gg 1$ the linear dependence is evident and leads to the effective diffusion constant $D \equiv v_0^2/2\gamma$. This transition from ballistic to diffusive behavior at $t\gamma \sim 1$ is well known [46,47]. Though departures from this behavior have been observed in the motion of human keratinocytes and fibroblasts cells [43], the transition has been observed in experiments on micron-sized self-motile colloidal particles that use self-diffusiophoresis as a propelling mechanism [9].

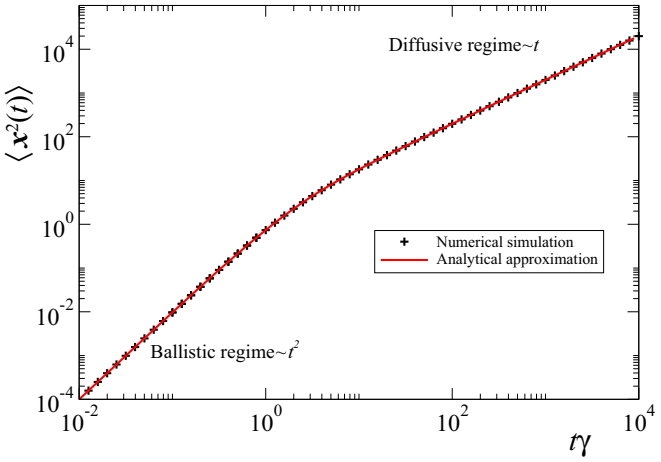

FIG. 1. (Color online) Mean-square displacement in units of $(v_0/\gamma)^2$ vs γt. The solid (red) line is the analytical approximation given by expression (16) and the data shown by symbols were obtained by averaging the numerical solution of Eqs. (2) considering 10^5 trajectories and integrating over 2×10^6 time steps.

B. Skewness and kurtosis

In contrast to the MSD, the next higher moments result in sensible parameters to measure the departure between our results given by Eq. (11) and those given by the TE (9) and those from the exact results given by numerical simulations. We refer to the skewness $\varkappa$ and the kurtosis κ, which have been used as a measure to test multivariate normal distributions [49] and are given explicitly by

$$\varkappa = \langle [(\boldsymbol{x} - \langle \boldsymbol{x}\rangle)\Sigma^{-1}(\boldsymbol{y} - \langle \boldsymbol{y}\rangle)^T]^3\rangle, \tag{17a}$$

$$\kappa = \langle [(\boldsymbol{x} - \langle \boldsymbol{x}\rangle)\Sigma^{-1}(\boldsymbol{x} - \langle \boldsymbol{x}\rangle)^T]^2\rangle, \tag{17b}$$

where $\boldsymbol{x}^T$ and $\boldsymbol{y}$ denote the transposed vector and an independent identically distributed vector to $\boldsymbol{x}$, respectively, and Σ is the matrix defined by the average of the dyadic product $(\boldsymbol{x} - \langle \boldsymbol{x}\rangle)^T \cdot (\boldsymbol{x} - \langle \boldsymbol{x}\rangle)$. For circularly symmetric distributions Σ^{-1} is diagonal and averages of odd powers of $\boldsymbol{x}$ entries vanish, thus leading to

$$\varkappa = 0, \tag{18a}$$

$$\kappa = 4\frac{\langle |\boldsymbol{x}|^4\rangle_{\rm rad}}{\langle |\boldsymbol{x}|^2\rangle_{\rm rad}^2}, \tag{18b}$$

where $\langle\cdot\rangle_{\rm rad}$ denotes the average over the radial distribution $rP(r)$, i.e., $\int_0^\infty dr\, r\, P(r)(\cdot)$.

For two-dimensional Gaussian distributions κ takes the invariant value 8, i.e., $\kappa = 8$, independently of the width and mean of the distribution. This occurs, for instance, for the marginal distribution $P(\boldsymbol{x},t)$ of the underdamped Brownian particle of Ornstein and Uhlenbeck (see [48]) for which the MSD corresponds to (16) and a kurtosis value of 8 for all times. On the other hand, it can be shown, following the lines in Appendix B, that the circularly symmetric normalized solutions of the two-dimensional wave equation (with zero initial velocity) has a kurtosis value $\frac{8}{3}$.

We have from Eqs. (9) and (11) that the kurtosis in each case is given by (see Appendix B)

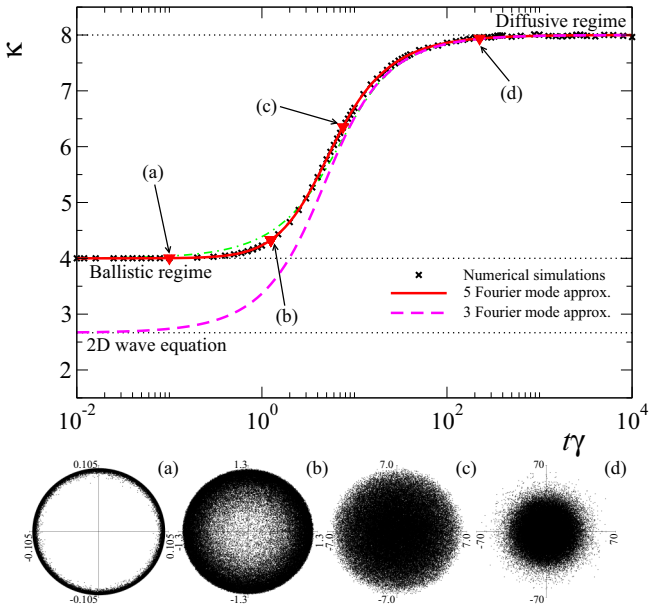

FIG. 2. (Color online) Kurtosis κ for the circularly symmetric solutions of the TE (9) (dashed magenta line), Eq. (11) (solid red line), and the exact solution obtained from numerical simulations of Eqs. (2) (crosses) vs $t\gamma$. Dotted lines mark the values 8, 4, and $\frac{8}{3} \simeq 2.6667$ that correspond to the values of κ for the two-dimensional Gaussian distribution, the two-dimensional distribution of particles that move with constant speed, and the circularly symmetric solutions of the two-dimensional wave equation, respectively. The insets show snapshots obtained from numerical simulations of the particles distribution $P_0(\boldsymbol{x},t)$ when they start to move from the origin at four different values of $t\gamma$, whose values of κ are characteristic (closed red triangles): (a) $t\gamma = 0.1$ and $\kappa = 4.003$, (b) $t\gamma = 1.25$ and $\kappa = 4.33$, (c) $t\gamma = 7.5$ and $\kappa = 6.352$, and (d) $t\gamma = 225$ and $\kappa = 7.938$ (the radius of the distribution has been scaled to fit the viewing area). Numerical simulations were performed by averaging 10^5 trajectories computed from Eqs. (2) and integrating over 2×10^6 time steps. The dash-dotted green line shows the time dependence of the kurtosis of the symmetric solution of the nonhomogeneous TE obtained in Ref. [30].

$$\kappa_3 = 8[\gamma^2 t^2 - 2\gamma t(2 + e^{-\gamma t}) + 6(1 - e^{-\gamma t})][\gamma t - (1 - e^{-\gamma t})]^{-2}, \tag{19a}$$

$$\kappa_5 = 8\left[\gamma^2 t^2 - 5\gamma t\left(\tfrac{3}{4} + \tfrac{1}{3}e^{-\gamma t}\right) + \left(\tfrac{87}{16} - \tfrac{49}{9}e^{-\gamma t} + \tfrac{1}{12^2}e^{-4\gamma t}\right)\right][\gamma t - (1 - e^{-\gamma t})]^{-2}, \tag{19b}$$

where the subindex denotes the number of Fourier modes retained. These results are compared with the exact calculation of κ in Fig. 2 (crosses). As expected, both descriptions and exact numerical calculations lead asymptotically to a Gaussian distribution since $\kappa \to 8$ as $\gamma t \to \infty$. On the other hand, in the short-time limit $\gamma t \ll 1$, a discrepancy between both descriptions is conspicuous. From the TE (9) the kurtosis of the distribution goes to $\frac{8}{3}$, which coincides with the value for the two-dimensional wave equation (the dashed magenta line in Fig. 2). However, from our numerical calculations, the time dependence of the kurtosis of the distribution of Brownian particles that move with constant speed acquires the value 4 for short times (the crosses in Fig. 2) and coincides with the kurtosis for the distribution that solves the generalized TE (11) (the solid red line) at all times.

Inset (a) in Fig. 2 shows a propagating ringlike distribution of particles at $t\gamma = 0.1$ for which $\kappa = 4.003$. Here κ rises as the ring starts to fill, as can be appreciated in inset (b), for which $t\gamma = 1.25$ and $\kappa = 4.33$. In inset (c) the ring is full and the distribution is approximately homogeneous on the disk. This is reflected in the value $\kappa = 6.352$ at $t\gamma = 7.5$ ($\kappa = \frac{16}{3} \simeq 5.333$ for a uniform distribution on a disk of given radius). At longer times the distribution becomes Gaussian, as indicated by the value $\kappa = 7.938$, as shown in inset (d) for $t\gamma = 225$.

It is worth pointing out that though the kurtosis calculated from the rotationally symmetric solutions of Eq. (11) coincides with the exact result computed from the Langevin equation (2), it does not show the characteristic hollow inside the ring in the short-time regime shown in inset (a) of Fig. 2. In fact, the solutions of related two-dimensional telegrapherlike equations, such as the one presented in this work (another is presented in Ref. [30] for the two-dimensional persistent random walk), show a *wake* effect that is characteristic of the solution of the two-dimensional wave equation [27]. In additional, although the solution of the inhomogeneous TE obtained in Ref. [30] does give the values $\kappa = 4$ and 8 at short and long times, respectively, it differs from our results in the intermediate regime, as is shown in Fig. 2 (the dash-dotted green line).

Realization of ensemble averages (such as those carried out in this paper) would be impractical in almost all realistic situations since too many trajectories would be required to have a good sample statistics. Thus, transport properties and/or other quantities such as the kurtosis shown in Fig. 2 can be extracted from trajectory data obtained using the camera-based single-particle tracking. However, as discussed in Ref. [45], inherent technical difficulties of the method introduce artifacts into the measurement results that are not properly taken into account when performing data analysis based on the MSD. An equivalent theory that considers higher moments has not been carried out and we believe that research to find good estimators to compute them from single-particle trajectories is required.

We finish this section by comparing the probability density distributions obtained in Fourier space in the short- and long-time regimes. Due to the simple appearance of the Laplace operator in Eqs. (9) and (11) and the symmetrical initial conditions, their respective solutions in Fourier space depend simply on $k = |\boldsymbol{k}|$. In the short-time regime, $\gamma t = 0.1$ in Fig. 3(a), the behavior of the solution to the TE (dashed magenta line) is close to that of the normalized solution to the two-dimensional wave equation (dashed gray line). Thus, those features attached to the solution of the two-dimensional wave equation are inherited by the two-dimensional TE. On the other hand, the solution to Eq. (11) (solid red line) departs conspicuously from that wavelike behavior, improving, as shown by the previous results, the description of particles that move with constant speed. In this regime, the equation satisfies the inhomogeneous wave equation $\partial_{tt}^2 P_0(\boldsymbol{x},t) = \frac{3}{4}v_0^2\nabla^2 P_0(\boldsymbol{x},t) + (v_0^2/4)Q(\boldsymbol{x})$ (see Appendix C), whose solution is given by (C6) and shown by the solid gray line in Fig. 3(a). We also show $\tilde{P}_0$ obtained from the numerical solution of Eq. (7) considering the first

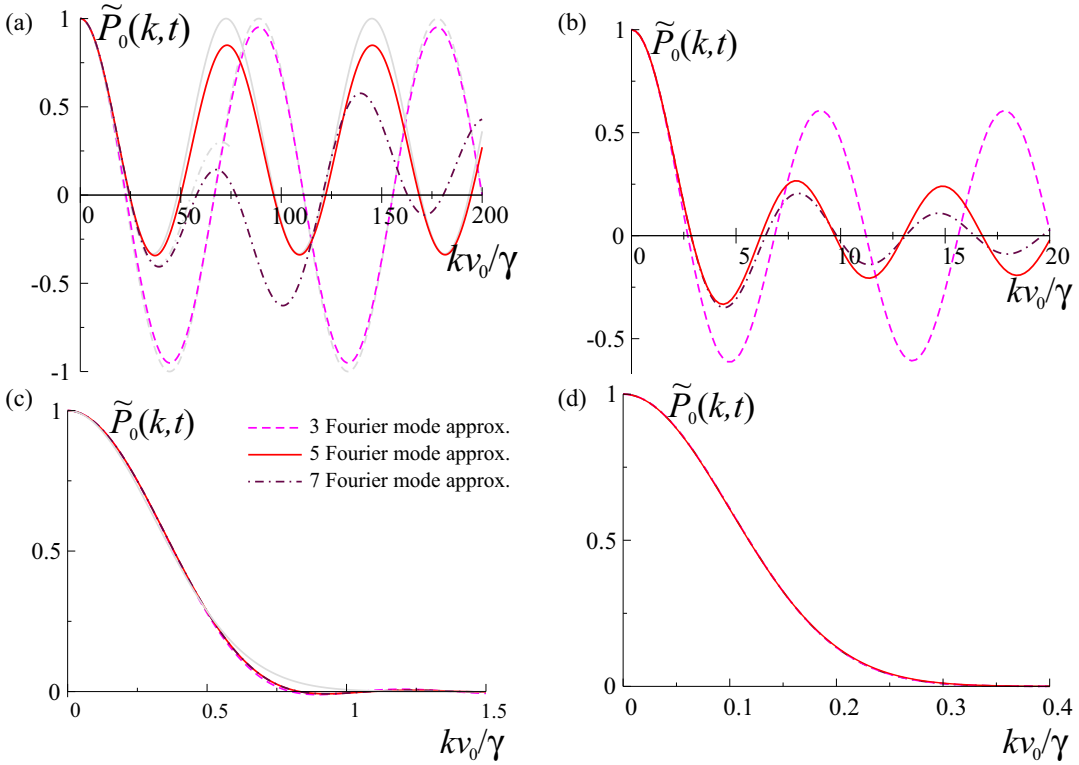

FIG. 3. (Color online) Plots showing the probability density $\tilde{P}_0(k,t)$ as a function of $k = |\boldsymbol{k}|$ at four different times, namely, (a) $\gamma t = 0.1$, (b) $\gamma t = 1$, (c) $\gamma t = 10$, and (d) $\gamma t = 100$. The solid red line corresponds to the solution of Eq. (11) and the dashed magenta line is the solution of the TE (9). The numerical solution, considering up to seven Fourier modes in Eq. (7), is shown by the dash-dotted line. In (a) the dashed gray line corresponds to the normalized solution to the two-dimensional wave equation with propagation speed $v_0\sqrt{2}$, namely, $\cos v_0 kt/\sqrt{2}$, and the solid gray line corresponds to the short-time limit of the Laplace inversion of expression (13) given by Eq. (C6).

seven Fourier modes (dash-dotted line). It is evident from Figs. 3(a) and 3(b) that more than five modes are needed to describe accurately the time evolution of $P_0(\boldsymbol{x},t)$ and we point out that $J_0(kv_0t)$, which corresponds to the two-dimensional Fourier transform of $\delta(|\boldsymbol{x}| - v_0t)/2\pi|\boldsymbol{x}|$, approximates well the seven-mode solution up to $kv_0t \simeq 50$.

At $\gamma t = 1$ [Fig. 3(b)] the solution to Eq. (9) departs from its wavelike behavior and starts to resemble the solution to Eq. (11), while the latter is qualitatively similar to the one provided by the seven-mode approximation. For longer times $\gamma t = 10, 100$ [Figs. 3(c) and 3(d), respectively], the three approximations shown are closer to each other and tend to a Gaussian distribution (solid gray line) that is the solution of the diffusion equation with the diffusion constant $v_0^2/2\gamma$.

V. CONCLUSION

Starting from a Langevin formalism to describe active particles that move in two dimensions with constant speed v_0, we obtained a Fokker-Planck equation for $P(\boldsymbol{x},\varphi,t)$, namely, the probability density of finding a particle at position $\boldsymbol{x}$ moving in direction $(\cos\varphi, \sin\varphi)$ at time t. By using Fourier transforms we obtained an infinite system of coupled ordinary differential equations for the Fourier modes $\tilde{P}_n(\boldsymbol{k},t)$. By a suitable transformation we were able to do a systematic analysis for different time regimes that tends towards a shorter-time description of the coarse-grained probability $P_0(\boldsymbol{x},t)$. Our formalism allows us, in principle, to obtain solutions arbitrarily close to the exact one by taking into account higher Fourier modes.

The long-time or diffusive approximation considers only the first three Fourier modes and lead to the well known TE (9) with a propagation speed $v_0/\sqrt{2}$. A shorter-time description that takes into account the next two Fourier modes leads to a generalized TE. Such an equation is inhomogeneous and the generalization relies on the non-Markovian nature of the diffusive term. A comparison between both approximations was made by computing the second and fourth moments of the circularly symmetric solutions of both equations, namely, the mean-square displacement and the kurtosis. The former did not exhibit a difference between the two descriptions and coincides with the exact result, while the latter, being a measure of the shape of the probability density, resulted in a sensible parameter in the short-time regime. However, despite the outstanding agreement between the numerical results and the kurtosis given by our generalization of the TE, the latter could not describe a shorter-time regime where sharp signals are transmitted as shown in inset (a) of Fig. 2.

From our analysis it is clear why the TE is not an appropriate model to describe the dynamics of Brownian particles that move with constant speed in the short-time regime, namely, only the three lowest modes of the Fourier expansion of the joint probability density $P(\boldsymbol{x},\varphi,t)$ are considered; however, the drift term $v_0\hat{\boldsymbol{v}}\cdot\boldsymbol{\nabla}P(\boldsymbol{x},\varphi,t)$ in (4) induces important correlations among the rest of the Fourier modes. Those

correlations are damped as the fluctuating direction of motion $[\cos\varphi(t), \sin\varphi(t)]$ becomes Gaussian distributed. The numerical calculation considering up to the first seven Fourier modes shows that in the short-time regime there exist strong correlations between the particle position and its direction of motion.

Although our description considers active point particles, our analysis can be extended to consider the diluted micron-sized systems of self-diffusiophoretic particles studied experimentally and theoretically in Ref. [44], where fluctuations of the rotational dynamics of the polar direction in which the particles move are separated from the fluctuations of the translational dynamics. Consideration of additional noise on the translational motion would induce a change in the transport properties at the short-time regime, exhibiting different behaviors in the MSD due to the competition of the different time scales involved. On the other hand, due to the intrinsic difference between two-dimensional rotations and the ones in three dimensions, it seems to be of interest to extend the present analysis to dimensions larger than 2.

We comment, in passing, that the appearance of memory in Eq. (11) makes it suitable to consider it as a candidate to describe anomalous diffusion phenomena as does a former generalization of the TE that uses fractional-time derivatives [50]. Indeed, if for the moment we disregard the inhomogeneous term, the mean-square displacement for arbitrary memory function $\phi(t)$ is

$$\langle \boldsymbol{x}^2(t)\rangle = 4v_0^2 \int_0^t ds\, e^{-\gamma(t-s)} \int_0^s ds' \int_0^{s'} ds''\phi(s''). \tag{20}$$

If the memory function $\phi(t)$ decays algebraically for long times as $t^{-\alpha}$, with $0<\alpha<1$, as does the Mittag-Leffler function $\tau^{-1}E_{\alpha,1}(-t^\alpha/\tau^\alpha)$ [where τ is a constant with units of time and $E_{\mu,\nu}(z)=\sum_{n=1}^{\infty} z^n/\Gamma(\mu j+\nu)$], the mean-square displacement can be expressed as

$$\langle \boldsymbol{x}^2(t)\rangle = 4\frac{v_0^2}{\tau}\int_0^t ds\, e^{-\gamma(t-s)} s^2 E_{\alpha,3}(-s^\alpha/\tau^\alpha), \tag{21}$$

which behaves superdiffusively $\sim t^{2-\alpha}$ in the asymptotic limit. Extensions of our analysis would consider colored noise and/or the effects of interactions among particles.

ACKNOWLEDGMENT

F.J.S. acknowledges support from DGAPA-UNAM through Grant No. PAPIIT-IN113114.

APPENDIX A: SECOND AND FOURTH MOMENTS OF THE CIRCULARLY SYMMETRIC INHOMOGENEOUS TERM $Q(\boldsymbol{x})$

If smooth circularly symmetric initial distributions of the form $P(\boldsymbol{x},\varphi,0)=\mathcal{X}(x)/(2\pi)^2$ are considered, with $x=|\boldsymbol{x}|$, expression (12) reduces simply to

$$Q(\boldsymbol{x}) = -\frac{1}{2\pi}\left[\frac{1}{x}\frac{\partial}{\partial x}\left(x\frac{\partial}{\partial x}\right)\right]\mathcal{X}(x) \tag{A1}$$

since the terms proportional to $\int_0^{2\pi} d\varphi\, e^{\pm i2\varphi}$ are zero. Thus, the factor $\beta=\int d^2\boldsymbol{x}\,\boldsymbol{x}^2 Q(\boldsymbol{x})$ that appears in (15b) is obtained by computing

$$\beta = -\int_0^\infty dx\, x^2\left[\frac{\partial\mathcal{X}(x)}{\partial x} + x\frac{\partial^2\mathcal{X}(x)}{\partial x^2}\right],$$

where the Laplacian in polar coordinates has been used. Integrating by parts once the second term in large square brackets and using boundary conditions $\mathcal{X}(x)|_{x=\infty}=0$ and $\frac{\partial\mathcal{X}(x)}{\partial x}|_{x=\infty}=0$ we get that

$$\beta = 2\int_0^\infty x^2\frac{\partial\mathcal{X}(x)}{\partial x}dx.$$

Integrating by parts again and using that $\int dx\, x\mathcal{X}(x)=1$ we finally arrive at the result

$$\beta = -4.$$

Analogously, the fourth moment is given by

$$\int_0^\infty dx\, x^4\left[\frac{\partial\mathcal{X}(x)}{\partial x} + x\frac{\partial^2\mathcal{X}(x)}{\partial x^2}\right] = 2^4\int_0^\infty dx\, x^3\mathcal{X}(x),$$

which gives zero for the localized initial condition $\mathcal{X}(x)=\delta(x)/x$.

APPENDIX B: KURTOSIS OF THE SOLUTIONS OF EQS. (9) AND (11)

Expressions (19) are obtained as follows. Equations (9) and (11) are multiplied by $x^4 x dx$ (recalling $x=|\boldsymbol{x}|$) and are integrated, over x, from 0 to ∞. For circularly symmetric solutions we get

$$\frac{d^2}{dt^2}\langle|\boldsymbol{x}|^4(t)\rangle_{\rm rad} + \gamma\frac{d}{dt}\langle|\boldsymbol{x}|^4(t)\rangle_{\rm rad} = 8v_0^2\langle|\boldsymbol{x}|^2(t)\rangle_{\rm rad}, \tag{B1a}$$

$$\frac{d^2}{dt^2}\langle|\boldsymbol{x}|^4(t)\rangle_{\rm rad} + \gamma\frac{d}{dt}\langle|\boldsymbol{x}|^4(t)\rangle_{\rm rad} = 4^2v_0^2\int_0^t ds\,\phi(t-s) \times\langle|\boldsymbol{x}|^2(s)\rangle_{\rm rad}, \tag{B1b}$$

respectively. As shown in Appendix A, the inhomogeneous term of Eq. (11) does not contribute if the initial condition corresponds to the case when all particles depart from the origin. The solutions to Eqs. (B1a) and (B1b), for vanishing initial conditions, are

$$\langle|\boldsymbol{x}|^4(t)\rangle_{\rm rad} = 8v_0^2\int_0^t ds\, e^{-\gamma(t-s)}\int_0^s ds'\langle|\boldsymbol{x}|^2(s')\rangle_{\rm rad}, \tag{B2a}$$

$$\langle|\boldsymbol{x}|^4(t)\rangle_{\rm rad} = 4^2v_0^2\int_0^t ds\, e^{-\gamma(t-s)}\int_0^s ds'\int_0^{s'} ds''\phi(s'-s'') \times\langle|\boldsymbol{x}|^2(s'')\rangle_{\rm rad}, \tag{B2b}$$

respectively. After substitution of the MSD (16) into (B2a) and (B2b) and performing the integration we get, for the kurtosis given by (18b), expressions (19).

APPENDIX C: APPROXIMATE SOLUTION OF EQ. (11)

The solution in the Fourier-Laplace domain to the generalization of the TE given by expression (13) can be computed by inverting the Green's function

$$\hat{G}(k,\epsilon) = \left\{\epsilon^2 + \gamma\epsilon + v_0^2k^2\left[\tfrac{3}{4} - \gamma(\epsilon+4\gamma)^{-1}\right]\right\}^{-1} \xrightarrow[\epsilon\ll 4\gamma]{} \left[\epsilon^2 + \gamma_k\epsilon + \frac{v_0^2k^2}{2}\right]^{-1}, \tag{C1}$$

where $\gamma_k \equiv (1 + \frac{v_0^2k^2}{2^4\gamma^2})\gamma$ and we have explicitly used that $\hat{\phi}(\epsilon) = \frac{3}{4} - \gamma(\epsilon+4\gamma)^{-1}$. By defining the k-dependent frequency $\omega_k^2 \equiv \frac{v_0^2k^2}{2} - (\frac{\gamma_k}{2})^2$, the Laplace inversion on the left-hand side can be carried out and (C1) is given by

$$\tilde{G}(k,t) \approx \frac{e^{-\gamma_k t/2}}{\omega_k}\sin\omega_k t \tag{C2}$$

for $4\gamma t \gg 1$. This approximate Green's function generalizes the corresponding one of the TE, which is obtained by setting $k = 0$ in γ_k, namely, $\tilde{G}^0(k,t) = e^{-\gamma t/2}\sin\omega_{0k}/\omega_{0k}$ with $\gamma = \gamma_{k=0}$ and $\omega_{0k} = (v_0^2k^2/2) - (\gamma/2)^2$.

By using (C2) we get

$$\begin{aligned}\tilde{P}_0(\boldsymbol{k},t) \approx{}& \frac{e^{-\gamma_k t/2}}{\omega_k}\left[\omega_k\cos\omega_k t + \left(\gamma - \frac{\gamma_k}{2}\right)\sin\omega_k t\right]\tilde{P}_0(\boldsymbol{k},0)\\ &+ \frac{v_0^2}{4}\tilde{Q}(\boldsymbol{k})\frac{e^{-\gamma_k t/2}}{\omega_k}\frac{e^{-(4\gamma-\gamma_k/2)t}\omega_k - \omega_k\cos\omega_k t + (4\gamma - \gamma_k/2)\sin\omega_k t}{(\gamma_k/2 - 4\gamma)^2 + \omega_k^2}.\end{aligned} \tag{C3}$$

Analytical inversion of the Fourier transform seems to be intractable by the appearance of k^4 in ω_k; however, for large space ranges, we have that to first order in $v_0^2k^2/2^4\gamma^2 \ll 1$, $\omega_k^2 \approx (v_0^2k^2/2)(1-2^{-4}) - (\gamma/2)^2$, which resembles its corresponding counterpart of the TE. With these considerations, the Green's function can be approximated further by $e^{-v_0^2k^2t/2^4\gamma}\tilde{G}^0(k',t)$, where $k' = \sqrt{15}k/2^2$. Thus the Green's function of the generalized TE in coordinate space can be written as

$$G(\boldsymbol{x},t) = \frac{1}{4\pi D't}\int d\boldsymbol{x}' e^{-(\boldsymbol{x}-\boldsymbol{x}')/4D't}G^0(\boldsymbol{x}',t), \tag{C4}$$

where $D' = v_0^2/2^4\gamma$.

On the other hand, in the short-time regime, expression (13) can be approximately written as

$$\hat{P}_0(\boldsymbol{k},\epsilon) = \frac{\epsilon\tilde{P}_0(\boldsymbol{k},0)}{\epsilon^2 + \frac{3}{4}v_0^2k^2} + \frac{v_0^2}{4}\frac{\tilde{Q}(\boldsymbol{k})}{\epsilon^2 + \frac{3}{4}v_0^2k^2}, \tag{C5}$$

from which, after inverting the Laplace transform, we obtain

$$\tilde{P}_0(\boldsymbol{k},t) = \tilde{P}_0(\boldsymbol{k},0)\left(\cos\frac{\sqrt{3}}{2}v_0kt + \frac{2}{3}\sin^2\frac{\sqrt{3}}{4}v_0kt\right), \tag{C6}$$

where we have imposed the rotational symmetry to write $\tilde{Q}(\boldsymbol{k}) = k^2\tilde{P}_0(\boldsymbol{k},0)$. The term $\cos\frac{\sqrt{3}}{2}v_0kt$ in expression (C6) is reminiscent of the solution of the wave equation with a speed of propagation $\sqrt{3}v_0/4$ larger than the value $v_0/\sqrt{2}$ given by the TE. It can be checked in a direct manner that expression (C6) satisfies the inhomogeneous wave equation

$$\frac{\partial^2}{\partial t^2}P_0(\boldsymbol{x},t) = \frac{3}{4}v_0^2\nabla^2P_0(\boldsymbol{x},t) + \frac{v_0^2}{4}Q(\boldsymbol{x}). \tag{C7}$$

[1] T. Vicsek and A. Zafeiris, Phys. Rep. **517**, 71 (2012).

[2] P. Romanczuk, M. Bär, W. Ebeling, B. Lindner, and L. Schimansky-Geier, Eur. Phys. J. Spec. Top. **202**, 1 (2012).

[3] E. A. Codling, M. J. Plank, and S. Benhamou, J. R. Soc. Interface **5**, 813 (2008).

[4] G. Viswanathan, M. da Luz, E. Raposo, and H. Stanley, *The Physics of Foraging: An Introduction to Random Searches and Biological Encounters* (Cambridge University Press, Cambridge, 2011).

[5] A. Cēbers and M. Ozols, Phys. Rev. E **73**, 021505 (2006).

[6] A. Y. Polishchuk, M. Zevallos, F. Liu, and R. R. Alfano, Phys. Rev. E **53**, 5523 (1996).

[7] S. A. Ramakrishna and N. Kumar, Int. J. Mod. Phys. B **16**, 3715 (2002).

[8] S. A. Ramakrishna and N. Kumar, Phys. Rev. E **60**, 1381 (1999).

[9] J. R. Howse, R. A. L. Jones, A. J. Ryan, T. Gough, R. Vafabakhsh, and R. Golestanian, Phys. Rev. Lett. **99**, 048102 (2007).

[10] H.-R. Jiang, N. Yoshinaga, and M. Sano, Phys. Rev. Lett. **105**, 268302 (2010).

[11] S. Bazazi, J. Buhl, J. J. Hale, M. L. Anstey, G. A. Sword, S. J. Simpson, and I. D. Couzin, Curr. Biol. **18**, 735 (2008).
[12] S. Bazazi, P. Romanczuk, S. Thomas, L. Schimansky-Geier, J. J. Hale, G. A. Miller, G. A. Sword, S. J. Simpson, and I. D. Couzin, Proc. R. Soc. London Ser. B **278**, 356 (2011).
[13] H. U. Bödeker, C. Beta, T. D. Frank, and E. Bodenschatz, Europhys. Lett. **90**, 28005 (2010).
[14] A. M. Edwards, R. A. Phillips, N. W. Watkins, M. P. Freeman, E. J. Murphy, V. Afanasyev, S. V. Buldyrev, M. G. E. da Luz, E. P. Raposo, H. E. Stanley *et al.*, Nature (London) **449**, 1044 (2007).
[15] J. Gautrais, C. Jost, M. Soria, A. Campo, S. Motsch, R. Fournier, S. Blanco, and G. Theraulaz, J. Math. Biol. **58**, 429 (2009).
[16] L. Li, E. C. Cox, and H. Flyvbjerg, Phys. Biol. **8**, 046006 (2011).
[17] T. Vicsek, A. Czirók, E. Ben-Jacob, I. Cohen, and O. Shochet, Phys. Rev. Lett. **75**, 1226 (1995).
[18] R. Golestanian, Phys. Rev. Lett. **108**, 038303 (2012).
[19] O. Chepizhko and F. Peruani, Phys. Rev. Lett. **111**, 160604 (2013).
[20] C. Weber, P. K. Radtke, L. Schimansky-Geier, and P. Hänggi, Phys. Rev. E **84**, 011132 (2011).
[21] C. Weber, I. M. Sokolov, and L. Schimansky-Geier, Phys. Rev. E **85**, 052101 (2012).
[22] P. K. Radtke and L. Schimansky-Geier, Phys. Rev. E **85**, 051110 (2012).
[23] G. H. Weiss and R. J. Rubin, in *Advances in Chemical Physics*, Vol. 52, edited by I. Prigogine and S. A. Rice (Wiley, New York, 1983), pp. 363–506.
[24] J. Masoliver, K. Lindenberg, and G. H. Weiss, Physica A **157**, 891 (1989).
[25] J. Masoliver and G. H. Weiss, Euro. J. Phys. **17**, 190 (1996).
[26] J. D. Barrow, Philos. Trans. R. Soc. London Ser. A **310**, 337 (1983).
[27] P. M. Morse and H. Feshbach, *Methods of Theoretical Physics, Part 1* (McGraw-Hill, New York, 1953).
[28] M. Boguñá, J. M. Porra, and J. Masoliver, Phys. Rev. E **58**, 6992 (1998).
[29] J. Masoliver, J. M. Porrà, and G. H. Weiss, Physica A **182**, 593 (1992).
[30] J. Masoliver, J. M. Porrà, and G. H. Weiss, Physica A **193**, 469 (1993).
[31] G. H. Weiss, Physica A **311**, 381 (2002).
[32] J. Masoliver and G. H. Weiss, Phys. Rev. E **49**, 3852 (1994).
[33] I. M. Sokolov and R. Metzler, Phys. Rev. E **67**, 010101(R) (2003).
[34] V. Kenkre and F. J. Sevilla, in *Contributions to Mathematical Physics: A Tribute to Gerard G. Emch*, edited by T. S. Ali and K. B. Sinha (Hindustan Book Agency, New Delhi, 2007), pp. 147–160.
[35] A. V. Plyukhin, Phys. Rev. E **81**, 021113 (2010).
[36] D. J. Durian and J. Rudnick, J. Opt. Soc. Am. A **14**, 235 (1997).
[37] D. J. Durian, Opt. Lett. **23**, 1502 (1998).
[38] A. Ishimaru, Appl. Opt. **28**, 2210 (1989).
[39] J. M. Porra, J. Masoliver, and G. H. Weiss, Phys. Rev. E **55**, 7771 (1997).
[40] S. Godoy and L. S. García-Colín, Phys. Rev. E **55**, 2127 (1997).
[41] G. Volpe, J. Buttinoni, D. Vogt, H. Kuemmerer, and C. Bechinger, Soft Matter **7**, 8810 (2014).
[42] H. Risken, *The Fokker-Planck Equation: Methods of Solution and Applications*, 2nd ed., Springer Series in Synergetics Vol. 18 (Springer, New York, 1989).
[43] D. Selmeczi, S. Mosler, P. H. Hagedorn, N. B. Larsen, and H. Flyvbjerg, Biophys. J. **89**, 912 (2005).
[44] X. Zheng, B. ten Hagen, A. Kaiser, M. Wu, H. Cui, Z. Silber-Li, and H. Lowen, Phys. Rev. E **88**, 032304 (2013).
[45] A. J. Berglund, Phys. Rev. E **82**, 011917 (2010).
[46] L. S. Ornstein, Proc. Acad. Amsterdam **21**, 96 (1919).
[47] R. Fürth, Z. Phys. **2**, 244 (1920).
[48] That is, $md\boldsymbol{v}/dt = -f\boldsymbol{v} + \boldsymbol{\xi}(t)$, where f is the friction constant and $\boldsymbol{\xi}(t)$ is a vector with Gaussian white noise entries. In this simple situation, the corresponding marginal probability density $P(\boldsymbol{x},t)$ results in a Gaussian distribution.
[49] K. V. Mardia, Sankhyā, Indian J. Stat. B **36**, 115 (1974).
[50] A. Compte and R. Metzler, J. Phys. A: Math. Gen. **30**, 7277 (1997).